

Article

Wide Strip Backfill Mining for Surface Subsidence Control and Its Application in Critical Mining Conditions of a Coal Mine

Wenhao Cao ¹, Xufeng Wang ^{1,2,3,*}, Peng Li ¹, Dongsheng Zhang ^{1,4}, Chundong Sun ⁵ and Dongdong Qin ¹

¹ School of Mines, China University of Mining & Technology, Xuzhou 221116, China; caowenhao0325@cumt.edu.cn (W.C.); lipeng@cumt.edu.cn (P.L.); zds@cumt.edu.cn (D.Z.); qindongdong@cumt.edu.cn (D.Q.)

² The Jiangsu Laboratory of Mining-Induced Seismicity Monitoring, China University of Mining & Technology, Xuzhou 221116, China

³ Key Laboratory of Deep Coal Resource Mining, China University of Mining & Technology, Xuzhou 221116, China

⁴ State Key Laboratory of Coal Resources and Safe Mining, China University of Mining & Technology, Xuzhou 221116, China

⁵ Jizhong Energy Handan Mining Industry Group, Handan 056002, China; sunchundong@cumt.edu.cn

* Correspondence: wangxufeng@cumt.edu.cn; Tel.: +86-159-5067-2601

Received: 31 December 2017; Accepted: 1 March 2018; Published: 5 March 2018

Abstract: Critical mining under buildings, railways, and water bodies (BRW) brings the contradiction between high recovery rate and minor environmental hazards. To lessen this contradiction, an innovative mining method referred to as “wide strip backfill mining” (WSBM) was proposed in this study. A Winkler beam model is applied to the primary key strata (PKS), and the study revealed a surface subsidence control mechanism and designed the technical parameters of the method. The respective numerical simulations suggested the feasibility of the proposed method and the main influencing factors on surface subsidence can be ranked in descending order as wide filling strip width (WFSW), filling ratio, and pillar width. Meanwhile, a drop in the WFSW from 96 m to 72 m brought out the surface subsidence reduction by 44.5%. By using the super-high water content filling material, the proposed method was applied in the Taoyi coal mine under critical mining conditions. The resulting surface subsidence and deformations met the safety requirements for building protection level 1, and the recovery rate reached 75.9%. Moreover, the application of the method achieved significant technical and economic benefits. The research can provide a theoretical and experimental substantiation for critical mining under BRW.

Keywords: critical mining; wide strip backfill mining; primary key strata; surface subsidence control; technical parameters; main influencing factors; wide filling strip width

1. Introduction

Vast reserves of coal resources worldwide are buried under buildings, railways, and water bodies (BRW), according to statistics, and these coal resources reach 25 billion tons in China [1], which is concentrated in densely-populated Eastern China. The exploitation of coal resources under BRW can prolong the life of old coal mines and ensure the sustainable development of mining areas but, at the same time, it will cause surface subsidence, and gradually bring a series of negative effects on the eco-environment and the safety of residents, including soil and water loss, damage to buildings, etc. [2–5].

To address the aforementioned issues, various mining methods have been applied to control surface subsidence. The room and strip mining can reach the goal to control the subsidence, but result in a vast waste of resources. Grout injection into bed separation is an effective measure against surface subsidence during longwall mining [6], however, the rigorous application conditions and technical level restrict its wide application. Backfill mining has gradually become the most effective method, which can reduce environmental hazards caused by surface subsidence, while ensuring a high recovery rate [7–11] in coal mining under BRW. However, because coal gangue and other wastes that can be reused to fill the mine-out area [12,13] are far less than the amount of coal mined, the shortage of filling material becomes particularly prominent. Despite the continuous development of paste materials in filling materials [14] and high water content materials [15], new problems emerge, such as complex filling systems, high filling cost, and the imbalance of excavating and backfilling, which largely restrict the development of backfill mining in coal mines, especially in areas with large stope under BRW.

When the stope is large enough, the mined area reaches the critical mining state [16]. Under these circumstances, it is difficult to control surface subsidence and obtain a high recovery rate from the use of a single method mentioned above [17]. Scholars introduced diversified composite mining methods allowing the strata structures, the filling bodies, and the coal pillars to jointly control the strata movement and reduce surface subsidence [18,19]. Based on the principles of subcritical extraction and partial extraction, filling strip mining was proposed, in which adjacent longwall panels were separated by stable pillars [20,21]. The intermittent cut-and-fill mining can successfully mitigate the overburden failure and subsidence, which contribute to addressing surface subsidence in critical mining [19]. Using the consolidated fill for backfilling the coal room and pillar mining goafs to mine out coal buried under buildings, the recovery rate increased by 28% [22]. The above research was more focused on the concepts. However, the surface subsidence control mechanism in critical mining was not thoroughly researched, and the composite methods were rarely applied to practice.

On the basis of previous research, in order to maximally exploit coal resources in critical mining, with the minimum economic cost and surface subsidence, this paper presents an innovative mining method called “wide strip backfill mining” (WSBM). The surface subsidence control mechanism of WSBM was analyzed by use of the key strata theory, and the technical parameters were designed in detail. The proposed method’s feasibility was verified via numerical simulation and its practical application was tested in the Taoyi coal mine of the Handan mining area, Hebei Province, China. Finally, the technical and economic benefits were compared with other methods. This study can provide the theoretical and experimental substantiation for critical mining under similar conditions.

2. Surface Subsidence Control of WSBM

2.1. A Brief Description

The layout of WSBM under critical or supercritical mining conditions under buildings is shown in Figure 1. According to the theory of rock stratum control, in general, when the ratio of the width of the mined area (or advancing distance) to the buried depth of the coal seam is in the range of 1.2 to 1.5, the mined area is defined as critical mining. When the value is larger than 1.5, the mined area is defined as supercritical mining [16].

The WSBM (Figure 2a) combining backfill mining and strip mining (Figure 2c) is a comprehensive method of subsidence control. It is applicable to large-scale (critical) coal extraction under BRW and high demand for surface subsidence control. As compared to longwall backfill mining (LBM), the WSBM method has larger pillars and smaller filling strips, of which the width of the filling strip exceeding that of the strip pillar by one to three times, so the filling strip is called wide filling strip (WFS). When the LBM method is adopted, more than one longwall backfilling face is needed at the critical extraction stage, while only small pillars are left between adjacent faces, or none at all (Figure 2b). Despite the slight decline in the recovery rate, the WSBM brings out less disturbance to the overburden, thus making a more efficient surface subsidence control possible. Moreover, the design of

appropriate WFSW will facilitate the coordination between mining and filling operations and thereby improve the production efficiency.

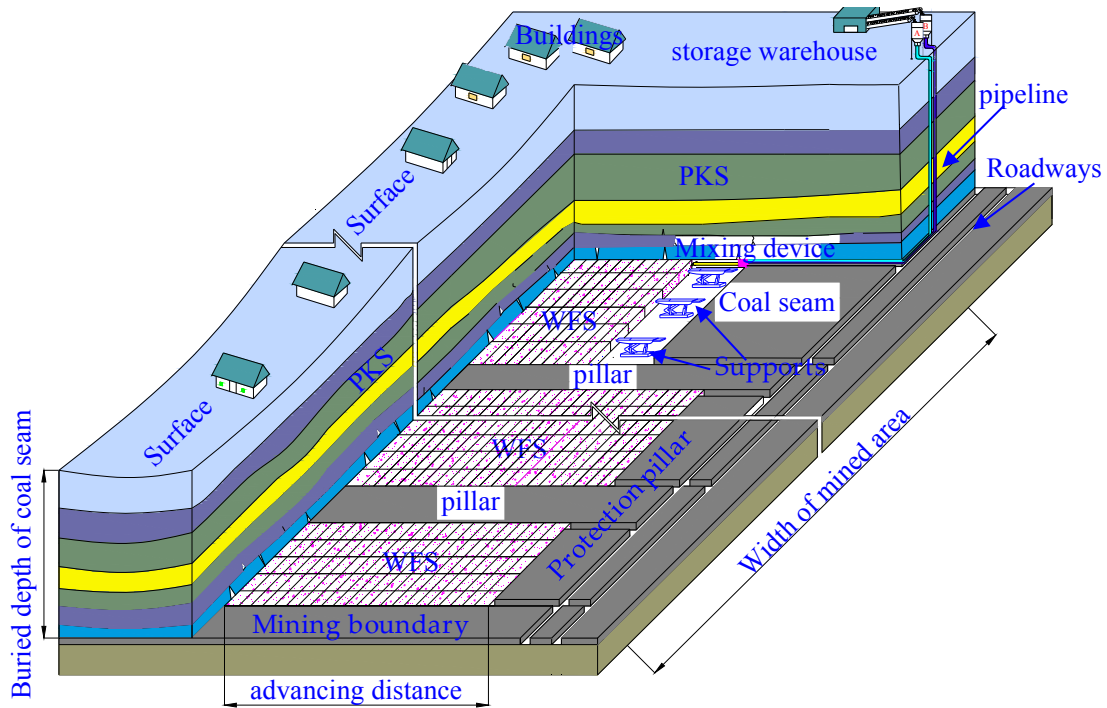


Figure 1. Layout of WSBM in critical mining under BRW.

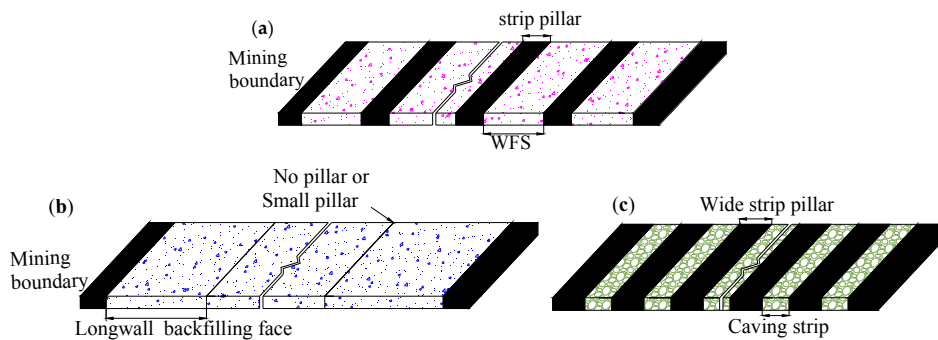


Figure 2. Layout at the critical extraction stage for three mining methods: (a) WSBM; (b) LBM; and (c) caving strip mining.

2.2. Surface Subsidence Control Mechanism

In WSBM, the space that allows the disturbed overburden to move and the height of the fracture zone in the overburden are smaller than those in caving mining. Additionally, the support provided by WFSs and coal pillars allows the roof strata to maintain continuity. Figure 3 depicts the structure of the overburden during WSBM.

When the mined area of WSBM is increased to infinity, the total load on WFSs and coal pillars approximates the weight of the overlying strata. In practice, the stope is a limited area. According to the key stratum theory, the stratum that controls the movement of the whole overburden strata is defined as the primary key strata (PKS), playing a controlling role in the deformation and breakage of the strata [23]. Thus, the overburden control imposed by the PKS can substantially reduce the load on WFSs and pillars.

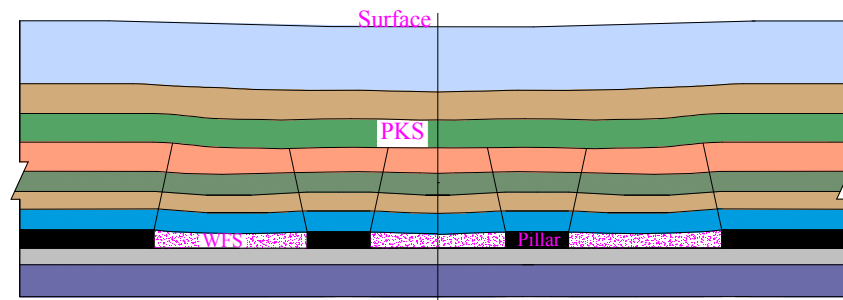


Figure 3. Structure of the overburden during WSBM.

2.2.1. Mechanical Model

A simplified beam model was constructed for the PKS (Figure 4a). Given the bilateral symmetry of the model, only one half of the PKS in the disturbed zone is analyzed (Figure 4b). As in [23], weak strata overlying the PKS are replaced by the equivalent load q_0 . During the WSBM process, the strata beneath the PKS are compacted and can be treated as an elastic foundation/bed of the Winkler type. According to the Winkler hypothesis, the subsidence at an arbitrary point of the elastic bed surface is directly proportional to the pressure at this point. The stress arising from the interaction between the PKS and underlying strata can be calculated by the following formula [24]:

$$\sigma_A = kw(x) \tag{1}$$

where σ_A is the support stress of the elastic foundation to PKS (kPa), $w(x)$ is the deflection of PKS (m); and k is the elastic bed coefficient (kPa/m).

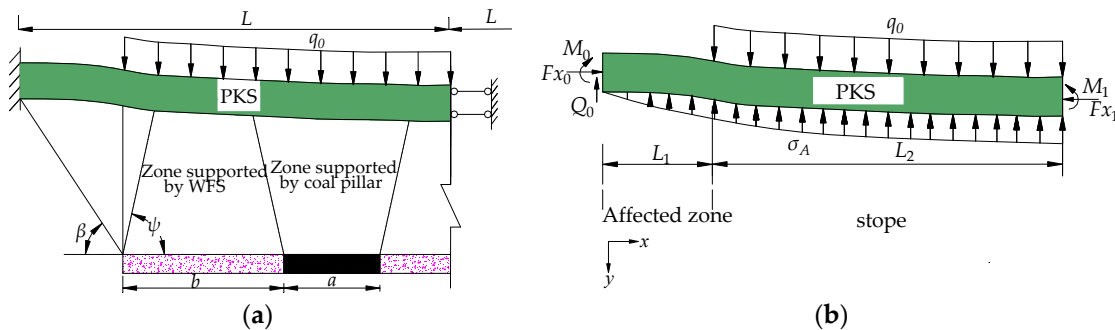


Figure 4. The model and equivalent stress of the PKS: (a) simplified model; and (b) stress analysis.

The equations governing the PKS deflection $w(x)$, are as follows:

$$\begin{aligned} EI \frac{d^4 w_1(x)}{dx^4} + kw_1(x) &= 0, -L_1 \leq x < 0 \\ EI \frac{d^4 w_2(x)}{dx^4} + kw_2(x) &= q_0, 0 \leq x \leq L_2 \end{aligned} \tag{2}$$

where EI is the flexural rigidity of the PKS, L_1 is the width of mining affected zone, $L_1 = \sum H_i \cot \beta$ (m); β is the limit angle; and H_i is thickness of strata above the coal seam (m).

Considering the beam boundary and symmetry conditions and defining that $\alpha = \sqrt[4]{\frac{k}{4EI}}$, the equations governing the PKS deflection can be simplified to the following form:

$$\begin{aligned} w_1(x) &= -M_0 \frac{\phi_3(\alpha x)}{EI\alpha^2} - Q_0 \frac{\phi_4(\alpha x)}{EI\alpha^3}, -L_1 < x < 0 \\ w_2(x) &= -M_0 \frac{\phi_3(\alpha x)}{EI\alpha^2} - Q_0 \frac{\phi_4(\alpha x)}{EI\alpha^3} + q_0/k(1 - \phi_1(\alpha(x - L_1))), 0 < x < L_2 \end{aligned} \tag{3}$$

By applying the respective equilibrium conditions, the bending moment M_0 and shear stress Q_0 at the left end of the beam can be obtained:

$$\begin{aligned} M_0 &= \frac{q_0}{a^2} \frac{\phi_1(\alpha L)\phi_4(\alpha L_2) - \phi_3(\alpha L)\phi_2(\alpha L_2)}{\phi_1(\alpha L)\phi_2(\alpha L) + 4\phi_3(\alpha L)\phi_4(\alpha L)} \\ Q_0 &= \frac{q_0}{a} \frac{\phi_4(\alpha L)\phi_4(\alpha L_2) + \phi_2(\alpha L)\phi_2(\alpha L_2)}{\phi_1(\alpha L)\phi_2(\alpha L) + 4\phi_3(\alpha L)\phi_4(\alpha L)} \end{aligned} \quad (4)$$

The Kirchoff function $\phi(x)$ is introduced in Equation (4), which can be expressed via hyperbolic and trigonometrical functions as follows [25]:

$$\begin{aligned} \phi_1(\alpha x) &= ch(\alpha x) \cos(\alpha x) \\ \phi_2(\alpha x) &= \frac{1}{2}[ch(\alpha x) \sin(\alpha x) + sh(\alpha x) \cos(\alpha x)] \\ \phi_3(\alpha x) &= \frac{1}{2}sh(\alpha x) \sin(\alpha x) \\ \phi_4(\alpha x) &= \frac{1}{4}[ch(\alpha x) \sin(\alpha x) - sh(\alpha x) \cos(\alpha x)] \end{aligned} \quad (5)$$

2.2.2. Deformation and Stability Conditions of the PKS

To satisfy the safety requirements of the buildings and structures located above the mining zone, it is necessary to limit the deformation of the PKS and exclude their fracture. The available research results [26] strongly suggest that the PKS and ground surface subside at the same rate. The maximum allowable values for surface deformation parameters, including those of the surface slope i_{\max} , curvature K_{\max} , and horizontal displacement ε_{\max} , depend on the safety requirements for specific categories of the buildings in question. During WSBM, the PKS maximum deflection should not exceed the maximum allowable surface subsidence [27]:

$$w(x)|_{x=L_2} \leq w_p = \min\left(ri_{\max}, \frac{r^2 K_{\max}}{1.52}, \frac{r\varepsilon_{\max}}{1.52b}\right) \quad (6)$$

where b is the coefficient of the surface horizontal displacement and r is the major radius of influence (m), which is the radial distance from the extraction well where drawdown is effectively zero for a given time.

To avoid PKS fracture, the following condition must be satisfied:

$$M_{\max} \leq W_z[\sigma] \quad (7)$$

where M_{\max} is the critical (maximum) bending moment that the PKS can bear without failure (kN·m), W_z is the bending resistance moment/section modulus of the PKS (m³), and $[\sigma]$ is the PKS ultimate tensile strength (MPa).

The above analysis implies that, during the WSBM process, the WFSs, coal pillars, and the PKS form a support system to control the surface subsidence. This mining method makes full use of the coordinated support provided by the PKS and the pillar-WFS composite support structure. It is possible to minimize the load acting on the pillar-WFS support structure by maximizing the load on the PKS while ensuring its stability. This is consistent with the principle of economic rationality and makes it possible to achieve the goals of subsidence reduction and recovery rate improvement.

3. Design of the Technical Parameters

The results of surface subsidence control depend on multiple factors, including the overburden structure, coal seam dip, mining height, stope size, mining method used, etc. The above mechanical model restricts the PKS motion to a relatively small space, with an adequate support being provided to satisfy its critical deformation and stability conditions. Therefore, the main factors influencing the surface subsidence of WSBM can be classified into two categories: (i) mining parameters, including WFSW and pillar width, and (ii) backfilling parameters, including the filling body strength and filling ratio (the ratio of the volume of the filling body to the volume of coal mined).

3.1. WFSW and Pillar Width

The surface subsidence control of WSBM requires the availability of at least one thick and hard rock layer in the overburden. The PKS identification was provided by using the original software package called KSPB which was developed in Xuzhou, China [28]. The limit span of the PKS can be calculated using a clamped-clamped beam model, and WFSW can be determined via the distance from the PKS to the coal seam and the inclination of fracture surface in the strata:

$$b \leq H_k \sqrt{2[\sigma]/q_0 + 2 \sum_1^t H_i / \tan \psi} \quad (8)$$

where b is WFSW (m), H_k and H_i are the thicknesses of the PKS (m) and the i th strata lying between the coal seam and the PKS, respectively, while ψ is the strata fracture angle.

Pillars are vital for the composite support structure and structural continuity of the PKS with large stopes. Figure 5 illustrates that the load acting upon a pillar is the sum of the load from the key strata and the weight of rocks within the zone supported by it.

$$P_c = (a + 2 \sum_1^t H_i \cot \psi) \sigma_A + \sum_1^t (a + 2 \sum_1^{t-1} H_i \cot \psi) \gamma_i H_i \quad (9)$$

Coal pillars are subjected to the triaxial compression during WSBM. According to the Wilson theory on the width of the plastic zone in coal pillars [29] and the Mohr-Coulomb failure criterion, the coal pillar ultimate strength should exceed the stress induced by the load acting on it to maintain stability:

$$P_{ct} = A(a - 0.00492Hm) \geq P_c \quad (10)$$

where a is a pillar (m), $A = \frac{2c \cos \phi}{1 - \sin \phi} + \frac{1 + \sin \phi}{1 - \sin \phi} \lambda \gamma H$ with H denoting the burial depth (m), c is the cohesion of the coal seam (MPa), ϕ is the angle of the internal friction of the coal, λ is the coefficient of lateral pressure on coal pillar, and m is the mining height (m).

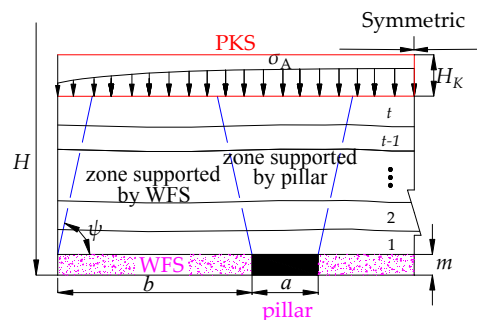


Figure 5. The support zone of the pillars and WFS.

3.2. The Filling Body Strength and Filling Ratio

The bearing capacity of WFSs and the effective space that allows overburden to move are mainly controlled by the filling body strength and filling ratio. The filling body strength is also used as a criterion for selecting filling materials. During WSBM, the ultimate compression of the filling body strength should exceed the stress induced by the maximum load acting on it:

$$[\sigma_f] \geq \sigma_{\max} = \sigma_A + \sum_1^t \gamma_i H_i \quad (11)$$

where σ_{\max} is the maximum stress on filling body (MPa), and γ_i is the bulk density of the i th strata (N/m³).

According to the theory of equivalent mining height [30], the effective space that allows the disturbed overburden to move during backfill mining is equivalent to the mining height of thin seams, and the equivalent mining height is the sum of the filling body compression and the unfilled height. The filling body compression depends on the external load, as well as the mechanical properties of the filling body. For a given filling ratio η , the equivalent mining height can be estimated by a joint usage of the stress-strain relationship for the filling body subjected to triaxial compression ($\varepsilon = f(\sigma)$) and criterion Equation (11), which yields the following expression:

$$M_e = m(1 - \eta) + m\eta f(\sigma_{\max}) \quad (12)$$

where M_e is equivalent mining height (m).

As soon as the surface subsidence is terminated, the relationship between the maximum allowable subsidence and equivalent mining height takes the following form:

$$M_e q \cos \alpha \leq w_p \quad (13)$$

where q denotes the coefficient of surface subsidence, which is calculated to the case of caving mining under critical conditions, while α is the coal seam dip.

The technical parameters for the main influencing factors can be derived from Equations (8)–(13). The technical parameters obtained are listed in Table 1.

Table 1. The technical parameters for the main influencing factors of WSBM.

No.	Main Influencing Factor	The Technical Parameter
1	WFSW	$b \leq H_k \sqrt{2[\sigma]/q_0} + 2 \sum_1^i H_i / \tan \psi$
2	Coal pillar width	$a \geq \frac{\sum_1^i H_i \cot \psi (2\sigma_A + \sum_1^i \gamma_i H_i) + 0.00492 H m A}{A - (\sigma_A + \sum_1^i \gamma_i H_i)}$
3	Filling body strength	$[\sigma_f] \geq (\sigma_A + \sum_1^i \gamma_i H_i)$
4	Filling ratio	$\eta \geq (1 - \frac{W_z}{mq \cos \alpha}) / [1 - f(\sigma_{\max})]$

Note: σ_A can be calculated using Formulas (1)–(7).

4. Numerical Simulation Analysis

To verify the reliability of the proposed mining method, numerical simulations of WSBM were performed using the software program FLAC3D, which is a numerical modeling code for advanced geotechnical analysis of soil, rock, and structural supports in three dimensions, which has been developed by the ITASCA Consulting group, Inc (Minneapolis, USA). An orthogonal experiment [31] was conducted to rank the main factors controlling the surface subsidence. The numerical simulations were based on the geological and technical conditions of the Taoyi coal mine of the Handan mining area, Hebei Province, China. A filling material with super-high water content was used.

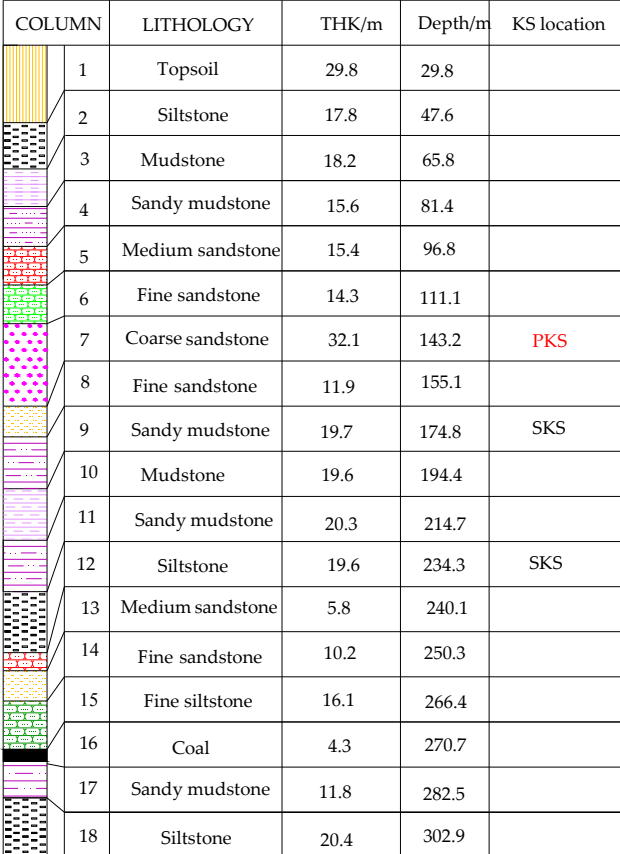
4.1. Determination of Parameters

The technical parameters for WSBM were determined based on the safety requirements for corresponding building category, geological and technical conditions, and the properties of the filling material. For building protection level 1, the appropriate values of i_{\max} , ε_{\max} , and K_{\max} are 3.0 mm/m, 2.0 mm/m, and 0.2 mm/m², respectively.

4.1.1. Geological and Mining Conditions

At the Taoyi coal mine, the limit angle is 55°, the strata fracture angle is 78°, and the coefficients of surface subsidence and horizontal displacement are 0.78 and 0.35, respectively. The stratigraphic

column of the #7 stope is shown in Figure 6. According to the results of the PKS and sub key strata (SKS) identification with the KSPB software, the PKS is 32.1 m-thick coarse sandstone, and its distances to the coal seam and the surface are 124 m and 110 m, respectively.



COLUMN	LITHOLOGY	THK/m	Depth/m	KS location
1	Topsoil	29.8	29.8	
2	Siltstone	17.8	47.6	
3	Mudstone	18.2	65.8	
4	Sandy mudstone	15.6	81.4	
5	Medium sandstone	15.4	96.8	
6	Fine sandstone	14.3	111.1	
7	Coarse sandstone	32.1	143.2	PKS
8	Fine sandstone	11.9	155.1	
9	Sandy mudstone	19.7	174.8	SKS
10	Mudstone	19.6	194.4	
11	Sandy mudstone	20.3	214.7	
12	Siltstone	19.6	234.3	SKS
13	Medium sandstone	5.8	240.1	
14	Fine sandstone	10.2	250.3	
15	Fine siltstone	16.1	266.4	
16	Coal	4.3	270.7	
17	Sandy mudstone	11.8	282.5	
18	Siltstone	20.4	302.9	

Figure 6. Stratigraphic column of the #7 stope.

4.1.2. Filling Material

In 2009, filling materials with super-high water content were used in the backfill mining in the Handan mining area, which was the first application of such materials in coal mining. This type of filling material has multiple advantages, such as high mobility, high strength at the early stage, and low filling cost per ton of extracted coal. A filling material with a volumetric water content of 95% has a triaxial compressive strength of 10 MPa and its stress-strain relationship for the triaxial compression conditions can be described by the following equation [32]:

$$\varepsilon = f(\sigma) = (-0.006\sigma^4 + 0.0624\sigma^3 - 0.0827\sigma^2 + 0.256\sigma) / 100 \quad (14)$$

The values of the major parameters for WSBM were estimated using the MATLAB program based on the geology of the Taoyi coal mine and the characteristics of the super-high water content material. The results obtained are listed in Table 2.

Table 2. Major factors controlling the WSBM process.

Maximum Allowable Subsidence W_z (mm)	WFSW, b (m)	Pillar Width, a (m)	Filling Ratio (%)	Triaxial Compressive Strength of Filling Body (MPa)
600	≤ 99.6	≥ 23.2	$> 84.9\%$	> 5.38

4.2. Experiment Scheme

4.2.1. Orthogonal Experimental Design

To reduce the filling cost, the strength of filling body can be excluded from the experiment as long as it meets basic requirements. Therefore, this orthogonal analysis included only the WFSW, pillar width, and filling ratio. Each factor was applied at three levels determined based on the values shown in Table 2, namely 96 m, 84 m, and 72 m for the WFSW; 24 m, 28 m, and 32 m for the pillar width; and 85%, 88%, and 91% for the filling ratio. The surface subsidence was used as the criterion for assessing the experimental results obtained.

4.2.2. Numerical Simulation Process

The simulated stope was designed to be 480 m (W_1) along the coal seam strike and 400 m (W_2) in the working face advance direction. The scope of the mined area reaches critical mining conditions with the buried depth of the coal seam of 266 m ($W/H = 1.5, 1.8$). The model boundary of 200 m and 240 m on both sides of the mining area was large enough to allow full-trough development without interference from the boundary conditions (allowable minimum boundary 186 m). To observe the surface subsidence, the model needs to be built to the surface. A numerical model with dimensions of 1200 m \times 1200 m \times 303 m was constructed containing 1,440,000 elements and 1,548,359 nodes in total, with a mesh size of the coal seam of 4 m \times 4 m (length \times width) and the roof to surface of 8 m \times 8 m. Displacement boundaries were applied to the four sides and bottom of the model, while no constraint was applied to the top surface. Mohr–Coulomb was selected as the constitutive model. Then surface subsidence was monitored along two observation lines at the top, which were along the strike and advance direction of the coal seam, respectively. The numerical simulation adopted sequential excavation and filling from panel 1 to panel 4. The FLAC3D model is schematically shown in Figure 7, while physical and mechanical parameters of rock lithology employed in the numerical simulations are listed in Table 3.

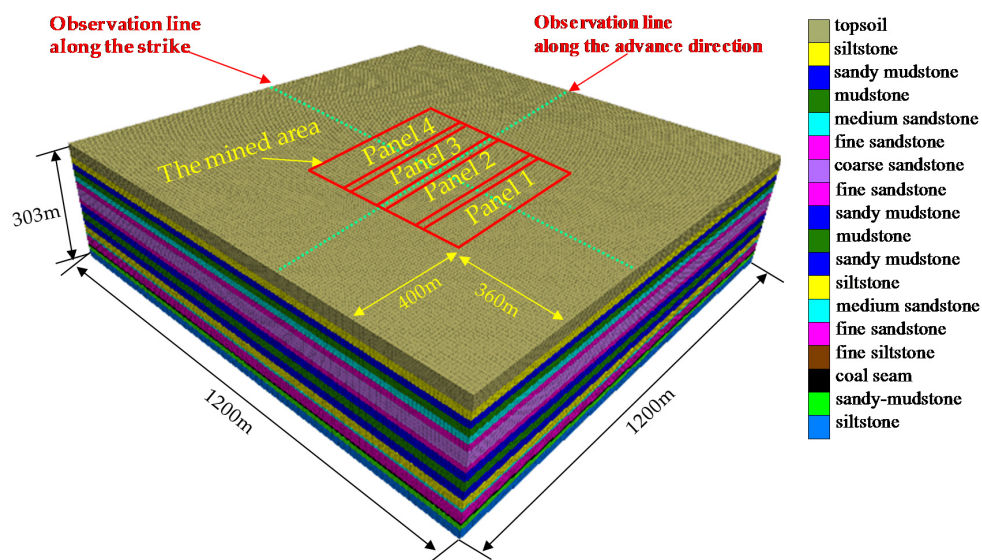


Figure 7. Establishment of the FLAC3D numerical model.

4.3. Results and Analysis

The simulation results are plotted in Figure 8 to illustrate the distribution of surface subsidence along the strike of the coal seam (higher than that along the advance direction). The orthogonal array constructed and the maximum surface subsidence observed in different scenarios are presented in

Table 4, where k_1 , k_2 , and k_3 refer to the average value, while “range” is a statistical measure of the coefficient of variation.

Table 3. Physical and mechanical parameters of rock lithology employed in the numerical simulations.

Lithology	Density ($\text{kg}\cdot\text{m}^{-3}$)	Bulk Modulus (GPa)	Shear Modulus (GPa)	Internal Friction Angle ($^\circ$)	Cohesion (MPa)	Tensile Strength (MPa)
Topsoil	1800	1.8	1.1	20	0.2	0.1
Sandy mudstone	2100	6.9	3.4	30	4.5	2.3
Medium sandstone	2530	8.0	6.8	37	3.8	3.1
Fine sandstone	2500	6.5	5.0	36	3.6	2.8
Coarse sandstone	2450	9.0	7.8	40	4.1	3.5
Siltstone	2300	7	6.4	30	2.1	2.5
Mudstone	2200	5.2	3.0	28	3.2	2.2
Fine siltstone	2350	7	3.8	35	3.0	1.8
2# coal seam	1400	4.2	2.5	30	1.0	2.0
the filling body	1250	4.0	2.1	28	1.2	1.5

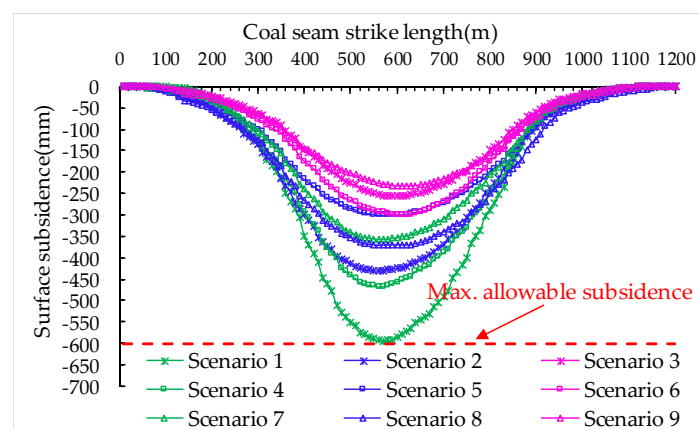


Figure 8. Distribution of surface subsidence along the seam strike for nine scenarios.

Table 4. L_9 (3^3) orthogonal array and experimental results.

Scenario	Factor			Maximum Surface Subsidence (mm)	Theoretical Equivalent Height (mm)	Equivalent Coefficient of Surface Subsidence q_e
	WFSW (m)	Pillar Width (m)	Filling Ratio			
1	96	24	85%	594.5	758.3	0.78
2	84	24	88%	430.7	621.9	0.69
3	72	24	91%	255.8	482.7	0.53
4	96	28	88%	468.3	625.7	0.75
5	84	28	91%	300.9	486.3	0.62
6	72	28	85%	300.0	740.4	0.41
7	96	32	91%	357.6	489.9	0.73
8	84	32	85%	370.7	743.7	0.50
9	72	32	88%	232.3	607.3	0.38
Surface subsidence						
k_1	473.5	427.0	421.7			
k_2	367.4	356.4	377.1			
k_3	262.7	320.2	304.8			
Range	210.8	106.8	116.9			
Equivalent coefficient of surface subsidence						
k_1	0.75	0.67	0.56			
K_2	0.60	0.59	0.61			
K_3	0.44	0.54	0.63			
Range	0.33	0.13	0.07			

Based on the theory of equivalent height, the compacted coal pillars and WFSs are considered as the floor, and the WSBM can be equivalent to the strip mining of a thin coal seam. The coefficient of surface subsidence in thin coal seam strip mining is approximately equal to that of caving mining under critical conditions. Therefore, the equivalent coefficient of surface subsidence q_e is introduced to describe the role of the PKS in WSBM:

$$q_e = w/M_e \cos \alpha \quad (15)$$

where w is the surface subsidence in WSBM (m), M_e can be calculated by Equations (12) and (14) (m), on the premise that the PKS works well. When q_e is less than q , it indicates that PKS plays a good supporting role; when q_e is greater than q , the compression of the WFSs-coal pillars floor exceeds the expected value, indicating that the instability of the PKS causes plate overload and a large amount of compression.

The equivalent coefficient of surface subsidence in different scenarios are presented in Table 4. The influence of different factors on surface subsidence and equivalent coefficient of surface subsidence in the orthogonal experimental are shown in Figure 9.

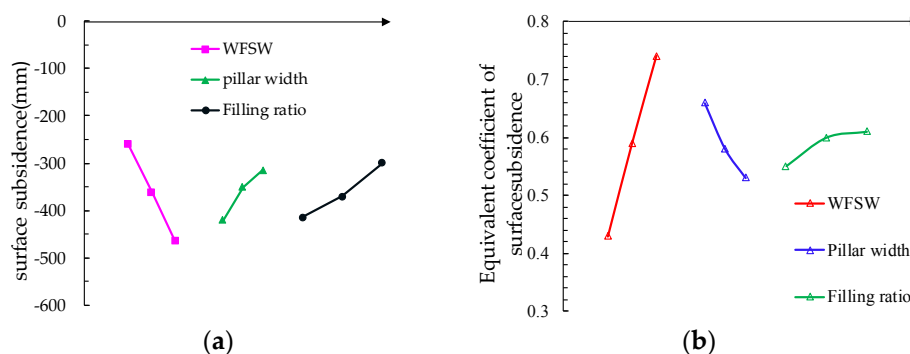


Figure 9. The influence of different factors on the targets in the orthogonal experimental: (a) the influence on surface subsidence; and (b) the influence on the equivalent coefficient of surface subsidence.

The analysis of the simulation results revealed the following:

- (1) The surface subsidence of the nine simulation schemes (shown in Figure 8) is less than the allowable subsidence (600 mm), which proves the rationality of the theoretical design. When the technical parameters of WSBM are critical values, the maximum surface subsidence volume is 594.5 mm. Therefore, the parameters need to be further optimized for reliability.
- (2) As shown in Figure 9a, the WFSW has a positive correlation with the surface subsidence, while the pillar width and filling ratio are negatively correlated with the surface subsidence. Based on the obtained range of the three factors influencing the surface subsidence (Table 4) in WSBM, they can be ranked in descending order of their effect as follows: the WFSW, filling ratio, and pillar width. With the WFSW decreasing from 96 m to 72 m, the maximum surface subsidence was reduced by 210.8 mm, or by 44.5%. Therefore, in order to meet the requirements of the surface control and improve its reliability, the reduction of WFSM can be given priority.
- (3) As shown in Figure 9b, the WFSW and filling ratio have a positive correlation with the equivalent coefficient of surface subsidence, while the pillar width is negatively correlated with the equivalent coefficient of surface subsidence. Among the three factors, the increase of the filling rate has no substantial effect on the surface subsidence coefficient. Therefore, based on the range of the factors influencing equivalent coefficient of surface subsidence in Table 4, they can be ranked in descending order as follows: the WFSW and pillar width. In order to avoid the failure of the PKS, the two factors of the WFSW and pillar width should be strictly controlled.

In summary, the surface subsidence in the numerical simulation met the requirement of surface subsidence control, indicating that WSBM can be applied to critical mining. The optimal combination of levels of the three factors is as follows: the WFSW of 72 m, pillar width of 24 m, and filling ratio of 91%. This set of parameters can efficiently control the surface subsidence in critical mining by making full use of the role that the PKS plays in supporting the overburden.

5. Case Studies

5.1. Study Area Overview

Taoyi coal mine is located in the Handan mining area, Hebei Province, China. There is a high density of villages on the surface of the mine, and local coal resources are all buried under villages. The #2 coal seam was mined, whose dip is 8°, and has an average mining height of 4.3 m. The experimental stope is located between #6 and #9 faults under the Tingsitou village and is protected by barrier pillars from both sides. Its specific location is shown in Figure 10.

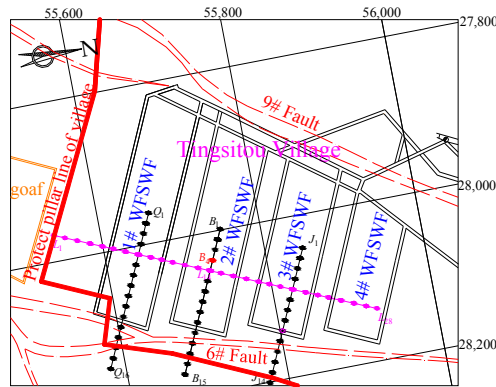


Figure 10. Location and layout of the stope.

Four WFSWFs were designed along the strike of the #2 coal seam. The WSBM method was implemented, by using super-high water content filling material and technical parameters of Scenario 8 (i.e., WFSW of 72 m, pillar width of 24 m, and filling ratio of 90%). To obtain the required filling ratio, the filling material was packed into bags before placement into goafs, as shown in Figure 11. Additionally, the support system was further reinforced by cross-wall support optimization and grouting for goafs via buried pipes. The resultant filling ratio was up to 92.3%, which exceeded the design value of 90% by 2.3%.

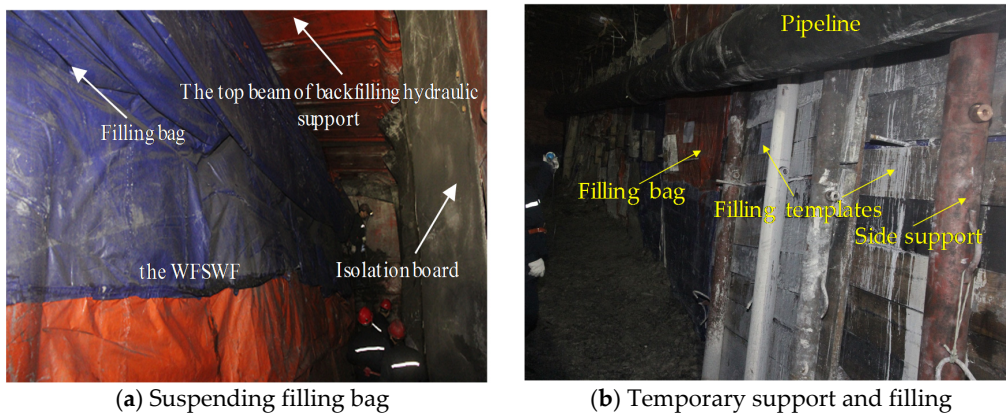


Figure 11. Bag-filling scheme for the experimental WFSWF.

5.2. Field Measurements

After implementation of the WSBM method, four observation lines were arranged on the surface above the stope, one running across the four WFSWFs in the strike direction (*L1–L28*), and the other three running in the dip direction (*Q1–Q16*, *B1–B15*, *J1–J14*). In total, 70 observation points were selected along these lines (Figure 10). Then, the surface subsidence at these points was periodically measured over a 15-month period. Table 5 shows the measured maximum surface subsidence and deformation values.

Table 5. Measured maximum surface subsidence and deformation values.

Site	Subsidence (mm)	Slope (mm/m)	Curvature (mm/m ²)	Horizontal Displacement (mm/m)
The WFSWF 1# to 4#	235	1.99	0.08	1.22

The experimental stope was 360 m (1.35 times the coal seam depth) in the strike direction and 250 m in the advance direction of the faces. The maximum surface subsidence corresponded to 235 mm, which satisfied the safety requirements for building protection level 1. This strongly suggests that the surface subsidence at the Taoyi coal mine was effectively controlled by the WSBM method. Moreover, a high recovery rate of 75.9% was achieved by this method.

5.3. Technical and Economic Benefits

To assess the advantages and possible drawbacks of the WSBM method, it was compared with other available mining methods based on their technical and economic benefits [33] when applied to the critical extraction coal mining under a village (see Table 6). The LBM method (with no pillars, or narrow ones) was found to provide the highest recovery rate, but it failed to ensure the required safety of building protection level 1, coordination between extraction and filling operations, or high efficiency in large-scale mining. The remaining three methods, including the proposed one, met the protection requirements for building protection level 1. However, strip mining, which is at odds with the principle of scientific and green mining, has a low recovery rate (below 50%). Partial/strip filling mining applies to short working faces with thin seams and a hard roof; its recovery rate is 50% to 80%, and its mining efficiency is medium. The proposed WSBM method ensures a high recovery rate, improved mining efficiency, and reasonable filling cost, which is accomplished by the use of super-high-water content filling material and the proper design of the working face length.

Table 6. Economic and technical benefits of different mining methods when applied to critical extraction coal mining under villages.

Mining Method	Face Length (m)	Recovery Rate	Efficiency of Mining	Filling Cost (USD)	Level of Building Damage
LBM	100–200	>90%	Medium	13–15	>Level I
Strip mining	<40	<50%	Low	—	<Level I
Partial/strip filling mining	40–80 m	50–80%	Medium	7–17	<Level I
WSBM	60–100	>75%	High	11–13	<Level I

Therefore, the WSBM can be treated as an improved method of strip filling mining. It is highly practical and can provide significant economic, technical, and environmental benefits, especially in cases where there are PKS in the overburden and the buildings and other important facilities on the ground require high levels of protection.

6. Discussion

This paper presents the WSBM method which can effectively control surface subsidence under critical mining conditions. Through the rational layout of WFSs and coal pillars, this method can make full use of the supporting role of the PKS and achieve the target of surface subsidence control. Simulation results showed that two key factors influencing the stability of the PKS are WFSW and coal pillar width. The technical parameters optimized by orthogonal tests were applied in the Taoyi coal mine under critical mining conditions in one direction, and the feasibility of the method was verified.

WSBM is the expansion and deepening of backfill mining method in critical mining. Compared with LBM, the factors influencing surface subsidence control are not only concentrated in the filling ratio and filling body strength, but also more important for the rational distribution of WFSs and coal pillars. Scholars carried out the preliminary study of backfilling with strip mining, and emphasized the importance of the retaining pillars through analyzing the influence of the retaining pillars on surface subsidence [21]. In this study, we found that when the coal pillar width reaches 24 m, continuing to increase its width, the effect of surface subsidence control has a slight improvement and, to some extent, the WFSW is a more important factor. This conclusion is beneficial to improve the coal recovery rate under critical mining conditions.

In addition, this paper made a comprehensive analysis of the factors influencing the surface subsidence, including WFSW, pillar width, and filling ratio, and deeply discusses the surface subsidence control mechanism, which has a good guidance and reference significance for critical mining.

It should be noted that the application of this WSBM requires the PKS existing above the coal seam, and the economic effect of WSBM will be greatly discounted, while being applied in sub-critical mining. The parameters, such as the coefficient of surface subsidence, limit angle, and strata fracture angle, are needed for a large number of field tests, which increases the difficulty in obtaining the technical parameters of the WSBM method. The limitation of the theoretical method is that the influence of filling technology on the surface subsidence cannot be quantitatively analyzed. The reliability of the numerical simulation method lies in the geometric accuracy of the model and the matching of the constitutive model. In this paper, the field application was sited between two faults (#6 and #9), and only the direction along the strike of the coal seam reached critical conditions; thus, the measured surface subsidence is less than in the numerical simulation. The surface subsidence control effect of the two directions at the same time reaching critical conditions is still to be further studied.

7. Conclusions

The results obtained make it possible to draw the following conclusions:

- (1) The WSBM method was proposed to control the surface subsidence and maximize the recovery rate in critical mining under BRW. The WSBM can control the surface subsidence through the coordinated support provided by the PKS and the pillar-WFS composite support structure while ensuring the stability of the PKS. By establishing the mechanical model of the PKS, the four technical parameters of WFSW, pillar width, filling ratio, and strength of the filling body were derived.
- (2) The performed numerical simulation via FLAC3D software suggested the reliability of the proposed method. The numerical simulation results ranked the three main influencing factors on the surface subsidence in descending order of their effect on surface subsidence as follows: the WFSW, filling ratio, and pillar width. As the WFSW decreased from 96 m to 72 m, the surface subsidence was reduced by 44.5%. In order to avoid the failure of the PKS, the two factors of the WFSW and pillar width should be strictly controlled.
- (3) The WSBM method using super-high water content filling material was applied as a pilot project at the Taoyi coal mine. For the preset WFSW of 72 m, pillar width of 24 m, and actual filling ratio of 92.3%, the measured surface subsidence and deformation met the safety requirements

for building protection level 1, while the recovery rate reached 75.9%. The field application demonstrated significant economic and technical benefits of the proposed method obtained in critical mining.

Acknowledgments: We acknowledge the financial support for this work, provided by the National Natural Science Foundation of China (grant no. 51474206, No. 51404254), the National Basic Research Program of China (973 Program—no. 2015CB162500), the Jiangsu Basic Research Program of China (BK20150051), and the Fundamental Research Funds for the Central Universities (2014QNA49).

Author Contributions: All authors contributed to this paper. Wenhao Cao prepared and edited the manuscript. Xufeng Wang and Peng Li participated in the formula derivation and numerical simulation processing during the research process. Dongsheng Zhang revised and reviewed the manuscript. Chundong Sun carried out extensive field test work and technical guidance. Dongdong Qin participated in the data collection and analysis processing.

Conflicts of Interest: The authors declare no conflict of interest.

Abbreviations

BRW	Buildings, railways, and water bodies
WSBM	Wide strip backfill mining
LBM	Longwall backfill mining
WFS	Wide filling strip
WFSW	Wide filling strip width
PKS	Primary key strata
SKS	Sub key strata
WFSWF	Wide filling strip working face

References

- Zhang, J.X.; Zhou, N.; Huang, Y.L.; Zhang, Q. Impact law of the bulk ratio of backfilling body to overlying strata movement in fully mechanized backfilling mining. *J. Min. Sci.* **2011**, *47*, 73–84. [[CrossRef](#)]
- Yang, D.J.; Bian, Z.F.; Lei, S.G. Impact on soil physical qualities by the subsidence of coal mining: A case study in Western China. *Environ. Earth Sci.* **2016**, *75*, 652.
- Tiwarly, R.K. Environmental impact of coal mining on water regime and its management. *Water Air Soil Pollut.* **2001**, *132*, 185–199. [[CrossRef](#)]
- Bell, F.G.; Genske, D.D. The influence of subsidence attributable to coal mining on the environment, development and restoration: Some examples from Western Europe and South Africa. *Environ. Eng. Geosci.* **2011**, *7*, 81–99. [[CrossRef](#)]
- Singh, K.B.; Dhar, B.B. Sinkhole subsidence due to mining. *Geotech. Geol. Eng.* **1997**, *15*, 327–341. [[CrossRef](#)]
- Xuan, D.Y.; Xu, J.L. Grout injection into bed separation to control surface subsidence during longwall mining under villages: Case study of Liudian coal mine, China. *Nat. Hazards* **2014**, *73*, 883–906. [[CrossRef](#)]
- Belem, T.; Benzaazoua, M. Design and application of underground mine paste backfill technology. *Geotech. Geol. Eng.* **2008**, *26*, 147–174. [[CrossRef](#)]
- Junker, M.; Witthaus, H. Progress in the research and application of coal mining with stowing. *Int. J. Min. Sci. Technol.* **2013**, *23*, 7–12. [[CrossRef](#)]
- Morteza, S. A review of underground mine backfilling methods with emphasis on cemented paste backfill. *Electron. J. Geotech. Eng.* **2015**, *20*, 5182–5208.
- Zhang, J.X.; Miao, X.X.; Guo, G.L. Development status of backfilling technology using raw waste in coal mining. *J. Min. Saf. Eng.* **2009**, *26*, 395–401.
- Zhang, J.X.; Zhang, Q.; Sun, Q.; Gao, R.; Germain, D.; Abro, S. Surface subsidence control theory and application to backfill coal mining technology. *Environ. Earth Sci.* **2015**, *74*, 1439–1448. [[CrossRef](#)]
- Bian, Z.F.; Miao, X.X.; Lei, S.G. The challenges of reusing mining and mineral-processing wastes. *Science* **2012**, *337*, 702–703. [[CrossRef](#)] [[PubMed](#)]
- Siriwardane, H.J.; Kannan, R.S.; Ziemkiewicz, P.F. Use of waste materials for control of acid mine drainage and subsidence. *J. Environ. Eng.* **2003**, *129*, 910–915. [[CrossRef](#)]
- Archibald, J.F.; Chew, J.L.; Lausch, P. Use of ground waste glass and normal Portland cement mixtures for improving slurry and paste backfill support performance. *CIM Bull.* **1999**, *92*, 74–80.

15. Feng, G.M. Research on the Super-High Water Packing Material and Filling Mining Technology and Their Application. Ph.D. Thesis, China University of Mining and Technology, Xuzhou, China, 2009.
16. Alejano, L.R.; Ramírez-Oyanguren, P.; Taboada, J. FDM predictive methodology for subsidence due to flat and inclined coal seam mining. *Int. J. Rock Mech. Min. Sci.* **1999**, *36*, 475–491. [[CrossRef](#)]
17. Chen, S.J.; Yin, D.W.; Cao, F.W.; Liu, Y.; Ren, K.Q. An overview of integrated surface subsidence-reducing technology in mining areas of China. *Nat. Hazards.* **2016**, *81*, 1129–1145. [[CrossRef](#)]
18. Kostecki, T.; Spearing, A.J.S. Influence of backfill on coal pillar strength and floor bearing capacity in weak floor conditions in the Illinois Basin. *Int. J. Rock Mech. Min.* **2015**, *76*, 55–67. [[CrossRef](#)]
19. Donovan, J.G.; Karfakis, M.G. Design of backfilled thin-seam coal pillars using earth pressure theory. *Geotech. Geol. Eng.* **2004**, *22*, 627–642. [[CrossRef](#)]
20. Xu, J.L.; Xuan, D.Y.; He, C.C. Innovative backfilling longwall panel layout for better subsidence control effect—Separating adjacent subcritical panels with pillars. *Int. J. Coal Sci. Technol.* **2014**, *3*, 297–305. [[CrossRef](#)]
21. Li, H.Z.; Guo, G.; Zhai, S.C. Mining scheme design for super high-water backfill strip mining under buildings: A Chinese case study. *Environ. Earth Sci.* **2016**, *75*, 1–12. [[CrossRef](#)]
22. Liu, J.W.; Sui, W.H.; Zhao, Q.J. Environmentally sustainable mining: A case study of intermittent cut-and-fill mining under sand aquifers. *Environ. Earth Sci.* **2017**, *76*, 562. [[CrossRef](#)]
23. Qian, M.G.; Miao, X.X.; Xu, J.L. Theoretical study of key stratum in ground control. *J. China Coal Soc.* **1996**, *21*, 225–230.
24. Jiang, H.Q.; Miao, X.X.; Zhang, J.X.; Liu, S.W. Gateside packwall design in solid backfill mining—A case study. *Int. J. Min. Sci. Technol.* **2016**, *26*, 261–265. [[CrossRef](#)]
25. Zhang, J.X.; Li, J.; An, T.L.; Huang, Y.L. Deformation characteristic of key stratum overburden by raw waste backfilling with fully-mechanized coal mining technology. *J. China Coal Soc.* **2010**, *35*, 357–362.
26. Li, Y.; Qiu, B. Investigation into Key Strata Movement Impact to Overburden Movement in Cemented Backfill Mining Method. *Procedia Eng.* **2012**, *31*, 727–733. [[CrossRef](#)]
27. Wang, X.F.; Zhang, D.S.; Sun, C.D.; Wang, Y. Surface subsidence control during bag filling mining of super high-water content material in the Handan mining area. *Int. J. Oil Gas Coal Technol.* **2016**, *13*, 87–102. [[CrossRef](#)]
28. Xu, J.L.; Qian, M.G. Method to distinguish key strata in overburden. *J. China Univ. Min. Technol.* **2000**, *29*, 463–467.
29. Wilson, A.H. Support load requirements on longwall faces. *Min. Eng.* **1975**, *134*, 479–491.
30. Guo, G.L.; Zhu, X.J.; Zha, J.F.; Wang, Q. Subsidence prediction method based on equivalent mining height theory for solid backfilling mining. *Trans. Nonferrous Metals Soc. China* **2014**, *24*, 3302–3308. [[CrossRef](#)]
31. Park, G.J.; Lee, T.H.; Lee, K.H.; Hwang, K.H. Robust design: An overview. *AIAA J.* **2006**, *44*, 181–191. [[CrossRef](#)]
32. Wang, X.F.; Qin, D.D.; Zhang, D.S.; Sun, C.D.; Zhang, C.G.; Xu, M.T.; Li, B. Mechanical characteristics of super high-water content material concretion and its application in longwall backfilling. *Energies* **2017**, *10*, 1592. [[CrossRef](#)]
33. Zhu, W.B.; Xu, J.M.; Xu, J.L.; Chen, D.Y.; Shi, J.X. Pier-column backfill mining technology for controlling surface subsidence. *Int. J. Rock Mech. Min. Sci.* **2017**, *96*, 58–65. [[CrossRef](#)]

